Iran Polym J (2016) 25:1009–1019
DOI 10.1007/s13726-016-0487-8

ORIGINAL PAPER

Reusability and selective adsorption of Pb^{2+} on chitosan/P(2-acryl amido-2-methyl-1-propanesulfonic acid-*co*-acrylic acid) hydrogel

Jie Yu[1] · Jidong Zheng[1] · Quanfang Lu[1,2] · Shuxiu Yang[1] · Xing Wang[1] · Xiaomin Zhang[1] · Wu Yang[1]

Received: 6 July 2016 / Accepted: 25 October 2016 / Published online: 1 November 2016

Abstract Reusability and selective adsorption toward Pb^{2+} with the coexistence of Cd^{2+}, Co^{2+}, Cu^{2+} and Ni^{2+} ions on chitosan/P(2-acrylamido-2-methyl-1-propanesulfonic acid-*co*-acrylic acid) [CS/P(AMPS-*co*-AA)] hydrogel, a multi-functionalized adsorbent containing $–NH_2$, –OH, –COOH and $–SO_3H$ groups was studied. The CS/P(AMPS-*co*-AA) was prepared in aqueous solution by a simple one-step procedure using glow discharge electrolysis plasma technique. The reusability of adsorbent in HNO_3, EDTA-2Na and EDTA-4Na was investigated in detail. The competitive adsorption of the metal ions at the initial stage was compared between their equal mass concentration and equal molar concentration. In addition, the adsorption mechanism of the adsorbent for adsorption of Pb^{2+} was also analyzed by XPS. The results showed that the optimum pH of adsorption was 4.8, and time of adsorption equilibrium was about 180 min. Adsorption kinetics fitted well in the pseudo second-order model. The equilibrium adsorption capacities of Pb^{2+}, Cd^{2+}, Co^{2+}, Cu^{2+}, and Ni^{2+} at pH 4.8 were obtained as 673.3, 358.3, 176.7, 235.0 and 171.7 mg g^{-1}, in their given order. The adsorbent displayed an excellent reusability using 0.015 mol L^{-1} EDTA-4Na solution as the eluent, and the desorption ratio could not correctly reflect the true characteristics of adsorption/desorption process. Moreover, the adsorbent showed good adsorption selectivity for Pb^{2+}. The molar adsorption capacity at the initial stage with equal molar concentration was more reliable than the mass adsorption capacity during the study of selective adsorption. According to the XPS results, the adsorption of Pb^{2+} ions by the CS/P(AMPS-*co*-AA) absorbent could be attributed to the coordination between N atom and Pb^{2+} and ion-exchange between Na^+ and Pb^{2+}.

Keywords Chitosan-based hydrogel · Reusability · Selective adsorption · Adsorption mechanism · Lead ions

Introduction

Heavy metals are usually found in many chemical and industrial effluents. Most these metals are carcinogenic or toxic and hence pose a threat to the environment and human health even at very low concentration [1]. Therefore, an effective control of industrial emissions and recovery of the heavy metal pollutants are significant industrial challenges and have become important issues for the environment and human health [2].

For a few decades, many methods have been developed and used for water treatment of heavy metals, such as reverse osmosis, membrane processes, electrochemical techniques, reduction and precipitation, biological treatments, ion-exchange and adsorption. Among them, adsorption is generally regarded as one of the versatile, effective and promising water treatment methods due to its simplicity of

Electronic supplementary material The online version of this article (doi:10.1007/s13726-016-0487-8) contains supplementary material, which is available to authorized users.

✉ Jie Yu
yujie741008@163.com

✉ Quanfang Lu
luqf@nwnu.edu.cn

[1] Key Lab of Bioelectrochemistry and Environmental Analysis of Gansu Province, College of Chemistry and Chemical Engineering, Northwest Normal University, Lanzhou 730070, People's Republic of China

[2] Editorial Department of the University Journal, Northwest Normal University, Lanzhou 730070, People's Republic of China

design, ease operation, and high efficiency [3, 4]. Besides, adsorption can also be used to recover valuable chemicals in industrial waste streams [5]. Over the past 20 years, activated carbon has been the most ubiquitous adsorbent for the removal of heavy-metal ions and other species because of its high surface area. However, the low adsorption capacity, considerably expensive cost, and laborious regeneration and selectivity have made its application less economically attractive. Therefore, the development of novel adsorbents with low cost [6] and high performance has remained as one of the hottest topics in water treatment.

Chitosan (CS) is a natural polysaccharide with many inherent advantages, such as natural abundance, biocompatibility and biodegradability. Due to the reactivity of amine groups (stable chelation sites) and hydroxyl groups, CS and its derivatives have been employed as adsorbents of heavy metals because of high adsorption capacity, promising reusability and excellent selectivity. However, dissolubility in acidic media limits its industrial-scale application because practical industrial effluents containing precious metal are extremely acidic and complex. Therefore, modification of CS to improve its solubility at acidic solution has both practical and technological significance. Recently, multi-functionalized polymeric hydrogels as adsorbents with ion-exchange and chelating capabilities are widely used for removing heavy metals. CS is a renewable and high-performance biopolymer which has gained considerable interest to prepare chitosan-based hydrogels as good candidates for adsorption [5]. Furthermore, chemical modifications can also improve the adsorption selectivity of CS.

In recent years, modified CS has been widely discussed in wastewater treatment. This material showed an excellent adsorption selectivity for highly toxic (Hg [7], Cr [8] and Cu [9]), weakly radioactive (U [10]), precious metal (Ag [11–13], Pd [14], Au [15]) and rare earth (Gd [16]) metal ions, etc. [17]. Generally speaking, the selective adsorption tests were carried out in mixture solution with the equal initial mass concentration [10, 18] or molar concentrations [7, 13] of each metal ion, and the selectivity was revealed by comparing with mass adsorption capacities (mg g^{-1}) [13, 17] or molar adsorption capacities (mmol g^{-1}) [11]. However, there is no unified unit for study on selectivity. In addition, the effects of pH and initial concentration on the selective adsorption have been widely investigated, but the kinetic behavior of selective adsorption has been rarely studied.

Adsorption–desorption is one of the most important phenomena to examine the recovery of metals adsorbed on the adsorbent and the regeneration of the adsorbent for subsequent reuse [19]. Therefore, choosing suitable eluent is very meaningful. So far, the applied eluents have been deionized water [19], acids (HCl [16] and HNO_3 [10]), bases (NaOH [20]), inorganic salts (NaCl, KCl and NH_4Cl) [19], organic chelating agents (EDTA [21–23] and acidified thiourea [14]), and their mixture components. In general, acids and EDTA show higher desorption capacities than water, bases and inorganic salts. However, the required concentration of acid is very high [19] that will corrode equipment in desorption process. EDTA has low solubility and does not make the adsorbent recovery fully [24], especially for a neutralized hydrogel adsorbent. Thus, this will affect the next adsorption. So finding new eluent is imperative.

Glow discharge electrolysis plasma (GDEP) is a kind of non-equilibrium plasma, which can generate intense UV radiation, shock waves, and a large number of energetic species such as H·, HO·, O·, HO_2· and H_2O_2 in aqueous solutions [25]. These active species would initiate the polymerization reaction [26]. Compared with the other initiation techniques (chemical initiation, UV-curing technique, and radiation), the advantage of GDEP is to lower the cost of setup, simple steps, mild conditions, controllable reaction and no second pollution [25–27].

In this work, the chitosan/P(2-acrylamido-2-methyl-1-propanesulfonic acid-*co*-acrylic acid) [CS/P(AMPS-*co*-AA)] hydrogel as a multi-functionalized adsorbent containing $–NH_2$, –OH, –COOH and $–SO_3H$ groups. This hydrogel was prepared in aqueous solution by a simple one-step method using GDEP technique, in which *N,N′*-methylene-bis-acrylamide (MBA) was used as a cross-linking agent. The thermal stability, morphology and structure of the adsorbent such as CS/P(AMPS-*co*-AA) were, determined by their corresponding techniques: TG-DTG, SEM and FTIR (Figs. S1–S3 are presented in supplementary material). In the next step, we focused on the study of reusability and selective adsorption toward Pb^{2+} with the coexistence of Cd^{2+}, Co^{2+}, Cu^{2+} and Ni^{2+} on the [CS/P(AMPS-*co*-AA)] hydrogel. The effects of pH and adsorption time on adsorption capacities were optimized batch-wise. The desorption and reusability behaviors of the adsorbent in various eluents, such as 0.5 mol L^{-1} HNO_3, 0.015 mol L^{-1} EDTA-2Na and 0.015 mol L^{-1} EDTA-4Na, were investigated in detail to explore the possibility for practical applications. The competitive adsorptions of Pb^{2+}, Cd^{2+}, Co^{2+}, Cu^{2+} and Ni^{2+} were based on their initial equal mass and molar concentrations. Moreover, the adsorption mechanism was elucidated by analyzing the XPS spectra of adsorbent before and after Pb^{2+} adsorption.

Experimental

Reagents

Chitosan (CS, 85% degree of deacetylation) was supplied by Zhejiang Golden Shell Biological Chemistry Co., Ltd, Zhejiang, China. Acrylic acid (AA, analytical grade,

Tianjin Guangfu Fine Chemical Research Institute, Tianjin, China) was distilled under reduced pressure before use. 2-Acrylamido-2-methyl-1-propanesulfonic acid (AMPS, analytical reagent grade, Shangdong Shouguang Runde Chemical Co., Ltd, Shangdong, China) was used without further purification. *N,N′*-methylene-bis-acrylamide (MBA, chemical pure, Shanghai Chemical Reagent Corporation, Shanghai, China) was used as received. Other materials, such as, ethylenediaminetetraacetic acid disodium salt (EDTA-2Na), ethylenediaminetetraacetic acid tetrasodium salt (EDTA-4Na), $Pb(NO_3)_2$, $Ni(NO_3)_2.6H_2O$, $Co(NO_3)_2.6H_2O$, $Cu(NO_3)_2.3H_2O$, $Cd(NO_3)_2.4H_2O$, HNO_3, were all analytical reagent grades and supplied from Shanghai Chemical Reagent Corporation, Shanghai, China.

Preparation of CS/P(AMPS-*co*-AA) as the adsorbent

The experimental apparatus was similar to our previous work [27]. In a 250 mL three-neck flask, 0.9 g CS and 0.06 g of MBA were added into 40 mL of distilled water and dispersed for 20 min at 25 °C under stirring. Then, 2 g AMPS and 8 mL AA were simultaneously added into the above solution and stirred for 10 min at 75 °C. After that, two electrodes were immersed into the solution to start discharge at 470 V and 62 mA for 3 min. Then, the reaction mixture was stirred for additional 4 h at 75 °C, as a post-polymerization process of the free radical- initiated crosslinking copolymerization reaction [26], followed by cooling the product to 25 °C. The canary yellow product was cut into small pieces. Then, the –COOH and $–SO_3H$ groups of the product were neutralized with 1 mol L^{-1} NaOH solution to a degree of neutralization of about 80%. Finally, the product was washed three times with distilled water, dried in vacuum oven, milled through a 100-mesh sieve and obtained CS/P(AMPS-*co*-AA) adsorbent in a white solid powder form.

The swelling of CS/P(AMPS-*co*-AA) adsorbent in distilled water and heavy metal ions solution were about 132.2 and 5.0 g g^{-1}, respectively. Therefore, the swelling of CS/P(AMPS-*co*-AA) adsorbent was ignored during the study of adsorption process.

Characterizations of samples

X-ray photoelectron spectroscopy (XPS) of CS/P(AMPS-*co*-AA) adsorbent before and after adsorption of Pb^{2+} was recorded on a PHI-5702 X-ray photoelectron spectrometer (USA). Metal determination before and after adsorption was performed three times separately using Varian 715-ES ICP-OES (Varian Inc., USA). The pH measurement was performed with a pH-211 Model pH meter (Hanna, Italy).

Adsorption studies

Effect of pH on adsorption

The pH of heavy-metal ions solution was adjusted with 0.1 mol L^{-1} HNO_3. A mixture containing 0.03 g adsorbent and 100 mL heavy-metal ion solution (300 mg L^{-1}, pH 1.0–6.5) was shaken for 4 h with 140 r min^{-1}. The adsorption capacity (Q_t) was calculated by the following:

$$Q_t = \frac{(C_0 - C_t)V}{m}, \quad (1)$$

where Q_t (mg g^{-1}) is the adsorption capacity of heavy-metal ions at any time, C_0 and C_t (mg L^{-1}) are the concentrations of the metal ions at initial and any time, m (g) is the amount of adsorbent and V (L) is the volume of the aqueous solution.

Adsorption kinetics

A mixture containing 0.06 g CS/P(AMPS-*co*-AA) adsorbent and 200 mL heavy-metal ion solution (300 mg L^{-1}, pH 5.0) was shaken with 140 r min^{-1}. The concentration of heavy-metal ions was measured by ICP at certain intervals. The adsorption capacities of heavy-metal ions were calculated by Eq. (1).

Desorption and regeneration

Desorption experiment was implemented using 100 mL of 0.5 mol L^{-1} HNO_3, 0.015 mol L^{-1} EDTA-2Na and 0.015 mol L^{-1} EDTA-4Na solution as the eluent of desorption, respectively. A series of 0.03 g adsorbents were added into 100 mL of 300 mg L^{-1} Pb^{2+}, Cd^{2+}, Co^{2+}, Cu^{2+} and Ni^{2+} solution (pH 4.8) and shaken with 140 r min^{-1} for 4 h at 25 °C, respectively. Then, the concentration of heavy-metal ions was measured using ICP and the adsorption capacity was calculated according to the Eq. (1). In the next step, the adsorbent loaded with the Pb^{2+}, Cd^{2+}, Co^{2+}, Cu^{2+} and Ni^{2+} ions was moved into the eluent solution and stirred at 140 r min^{-1} for 4 h. The final heavy-metal ions concentration was measured by ICP. The desorption capacity was calculated from final heavy-metal ions concentration in the desorption medium. Consecutive adsorption–desorption experiments were repeated three times. The desorption ratio (η) was calculated from the following expression:

$$\eta = \frac{Q_d}{Q_a} \times 100\%, \quad (2)$$

where η (%) is desorption ratio, Q_d and Q_a (mg g^{-1}) are the desorption and adsorption capacities, respectively.

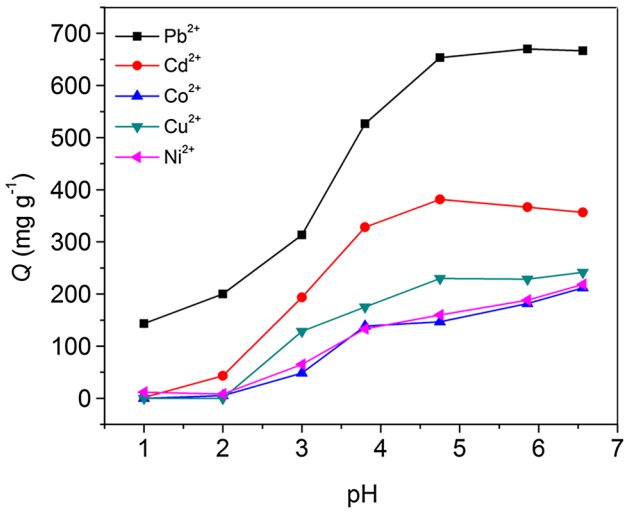

Fig. 1 pH versus adsorption for CS/P(AMPS-*co*-AA) for Pb^{2+}, Cd^{2+}, Co^{2+}, Cu^{2+}, and Ni^{2+} at 25 °C (initial solution 300 mg L^{-1})

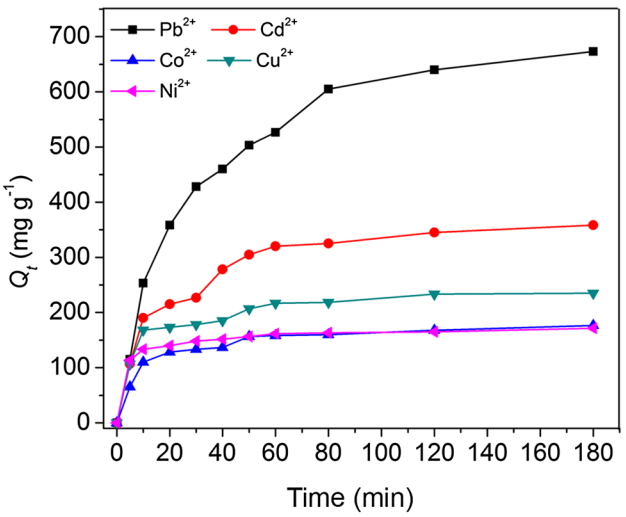

Fig. 2 Contact time versus adsorption for CS/P(AMPS-*co*-AA) for Pb^{2+}, Cd^{2+}, Co^{2+}, Cu^{2+}, and Ni^{2+} at pH 4.8 (initial solution 300 mg L^{-1})

Selective adsorption

The selective adsorption of heavy-metal ions containing equal mass concentration (i.e., 300 mg L^{-1}) and equal molar concentration (i.e., 1.45 mmol L^{-1}) of Pb^{2+}, Cd^{2+}, Co^{2+}, Cu^{2+} and Ni^{2+} ions were achieved at pH 4.8 and 25 °C. A series of 0.06 g adsorbents were added into 200 mL of mixture solution and shaken with 140 r min^{-1}. The concentration of heavy-metal ions was measured by ICP at certain intervals.

Results and discussion

Effect of pH on adsorption

The pH is one of the most important parameters, which affects the surface charge of the active adsorption sites and the degree of ionization. The adsorption of heavy-metal ions on the CS/P(AMPS-*co*-AA) adsorbent was investigated over the pH range 1.0–6.5 because heavy-metal ions could be precipitated by OH^- to form metal hydroxide above pH 6.5 [28]. Figure 1 shows the effect of pH on the adsorption capacity of the CS/P(AMPS-*co*-AA) adsorbent. There is a sharp increase of adsorption capacities when the pH is increased from 2.0 to 4.8; and it is not significantly altered beyond pH 4.8. At lower pH values (pH <2.0), protons compete with the metal ions for the active adsorption sites, and the sulfonate and carboxylate groups are protonated to block the chelation interaction between these groups and metal ions. In addition, the CS/P(AMPS-*co*-AA) adsorbent is in a collapsed and shrunken state [25]. As a result, it is difficult for metal ions to diffuse into the interior of adsorbent and the adsorption capacity is very low. With increasing the pH from 2.0 to 4.8, there is a drop in protonation of $–COO^-$ and $–SO_3^-$. Because of the electrostatic repulsive forces of $–COO^-$ and $–SO_3^-$, the adsorbent is in a small swelling state. This state benefits metal ions diffusion into the network to reach binding sites [19]. As a result, the adsorption capacity is increased. The pH also affects the metal solubility and speciation in aqueous solution, so the adsorbent has different adsorption capacities for Pb^{2+}, Cd^{2+}, Co^{2+}, Cu^{2+} and Ni^{2+}. Therefore, we chose pH 4.8 as the optimum adsorption pH value.

Adsorption kinetics

The effect of adsorption capacities of the adsorbent toward Pb^{2+}, Cd^{2+}, Co^{2+}, Cu^{2+} and Ni^{2+} on different contact times at pH 4.8 and 25 °C is illustrated in Fig. 2. It is obvious that the adsorption capacities increase sharply within 60 min, and begin to increase slowly from 60 to 120 min, and finally level off after 180 min. The equilibrium adsorption capacities of Pb^{2+}, Cd^{2+}, Co^{2+}, Cu^{2+} and Ni^{2+} are 673.3, 358.3, 176.6, 235 and 171.7 mg g^{-1}, in the corresponding order, implying that CS/P(AMPS-*co*-AA) adsorbent has high adsorption capacities and quite fast adsorption rates.

Adsorption kinetics describes how fast the adsorption occurs and also can give information on the factors affecting the reaction rate. To investigate the adsorption mechanism, the pseudo first- and second-order kinetic models were used to evaluate the experimental data [29, 30].

The pseudo first-order model assumes that the adsorption is originated from a physical process. It is represented as follows [29]:

Table 1 Adsorption kinetic parameters of CS/P(AMPS-*co*-AA) hydrogel adsorbent for Pb^{2+}, Cd^{2+}, Co^{2+}, Cu^{2+} and Ni^{2+} at pH 4.8 and 25 °C

Metal ions	$Q_{e,exp}$ (mg g^{-1})	Pseudo first-order model			Pseudo second-order model		
		k_1 (min^{-1})	$Q_{e,cal}$ (mg g^{-1})	R^2	$k_2 \times 10^{-4}$ (g mg^{-1} min^{-1})	$Q_{e,cal}$ (mg g^{-1})	R^2
Pb^{2+}	673.3	0.0246	575.8	0.9837	0.527	769.2	0.9974
Cd^{2+}	358.3	0.0266	257.2	0.9528	1.78	384.6	0.9970
Co^{2+}	176.7	0.0229	98.1	0.8622	5.45	184.2	0.9981
Cu^{2+}	235.0	0.0351	159.8	0.9343	4.72	245.7	0.9976
Ni^{2+}	171.7	0.0233	61.2	0.7619	12.4	173.9	0.9993

Table 2 Adsorption capacity, desorption capacity and desorption ratio of hydrogel for Pb^{2+}, Cd^{2+}, Co^{2+}, Cu^{2+} and Ni^{2+} in different eluents

Metal ions	0.5 mol L^{-1} HNO_3			0.015 mol L^{-1} EDTA-2Na			0.015 mol L^{-1} EDTA-4Na		
	Q_a (mg g^{-1})	Q_d (mg g^{-1})	η (%)	Q_a (mg g^{-1})	Q_d (mg g^{-1})	η (%)	Q_a (mg g^{-1})	Q_d (mg g^{-1})	η (%)
Pb^{2+}	653.3	653.3	100.0	651.7	635.0	97.4	653.3	601.6	92.1
Cd^{2+}	435.0	405.8	93.3	443.3	385.0	86.8	431.7	368.4	85.3
Co^{2+}	174.2	165.0	94.7	176.7	176.7	100.0	175.0	168.3	96.2
Cu^{2+}	210.0	203.3	96.8	226.7	196.7	86.8	201.7	193.4	95.9
Ni^{2+}	180.0	177.5	98.6	163.3	163.3	100.0	168.3	168.3	100.0

$$\lg (Q_e - Q_t) = \lg Q_e - \frac{k_1}{2.303} t, \tag{3}$$

where Q_e and Q_t (mg g^{-1}) are the adsorption capacities at equilibrium and at any time t (min), respectively. k_1 (min^{-1}) is the rate constant of pseudo first-order adsorption.

The pseudo second-order model is in accordance with the chemisorption mechanism being the rate-controlling step [30]. It is expressed as:

$$\frac{t}{Q_t} = \frac{1}{k_2 Q_e^2} + \frac{t}{Q_e}, \tag{4}$$

where k_2 (g mg^{-1} min^{-1}) is the rate constant of the pseudo second-order model.

The kinetic parameters are all listed in Table 1 (the models of linear plots of the pseudo first- and second-order are shown in Fig. S4 as supplementary material). It is obvious that pseudo second-order model agrees with the experimental data better than the pseudo first-order model. As can be seen from Table 1, the calculated $Q_{e,cal}$ values (Pb^{2+} 769.2, Cd^{2+} 384.6, Co^{2+} 184.2, Cu^{2+} 245.7, Ni^{2+} 173.9 mg g^{-1}) obtained from the pseudo second-order model are closer to the experimental $Q_{e,exp}$ values (Pb^{2+} 673.3, Cd^{2+} 358.3, Co^{2+} 176.7, Cu^{2+} 235.0, Ni^{2+} 171.7 mg g^{-1}) than those from the pseudo first-order kinetics $Q_{e,cal}$ values (Pb^{2+} 575.8, Cd^{2+} 257.2, Co^{2+} 98.1, Cu^{2+} 159.8, Ni^{2+} 61.2 mg g^{-1}). In addition, the R^2 values of the pseudo second-order model are closer to unity, and are higher than the pseudo first-order kinetics R^2 values. All these results suggest that the adsorption kinetics fit well to the pseudo second-order model. So the rate-limiting step in the adsorption process of metal ions onto CS/P(AMPS-*co*-AA) adsorbent is a chemisorption process which may involve the coordination and ion-exchange interactions between the heavy-metal ions and the binding sites of adsorbent [30].

Desorption and reusability

Adsorption–desorption is an important procedure to study the reusability of the adsorbent and the recovery of metal ions [19]. Preliminary experiments using distilled water for desorption studies did not show any heavy-metal ions recovery. This shows that the interaction between heavy-metal ions and adsorbent is very strong. Many papers reported that HNO_3 and EDTA solutions as eluents gave good desorption results (around 85%) for heavy-metal ions adsorbed onto modified chitosans, such as chitosan crosslinked with epichlorohydrin-triphosphate (CTS–ECT-TPP) [19], chitosan deads [24], functionalized chitosan [20], chemically and crosslinked chitosan [31], and so on. In this study, 0.5 mol L^{-1} HNO_3, 0.015 mol L^{-1} EDTA-2Na and 0.015 mol L^{-1} EDTA-4Na solutions were used as eluents for desorption of heavy-metal ions, respectively. The adsorption capacity, desorption capacity and desorption ratio of adsorbent for Pb^{2+}, Cd^{2+}, Co^{2+}, Cu^{2+} and Ni^{2+} in different eluents are listed in Table 2. It can be observed that all eluents possess the outstanding desorption capacity and the desorption ratio, over 85%, for Pb^{2+}, Cd^{2+}, Co^{2+}, Cu^{2+} and Ni^{2+}. This is reasonably attributed to the fact that the adsorbent contains one or more electron-donor atoms such as N and O that can form coordination bonds with heavy-metal ions [29–31]. Since EDTA-2Na

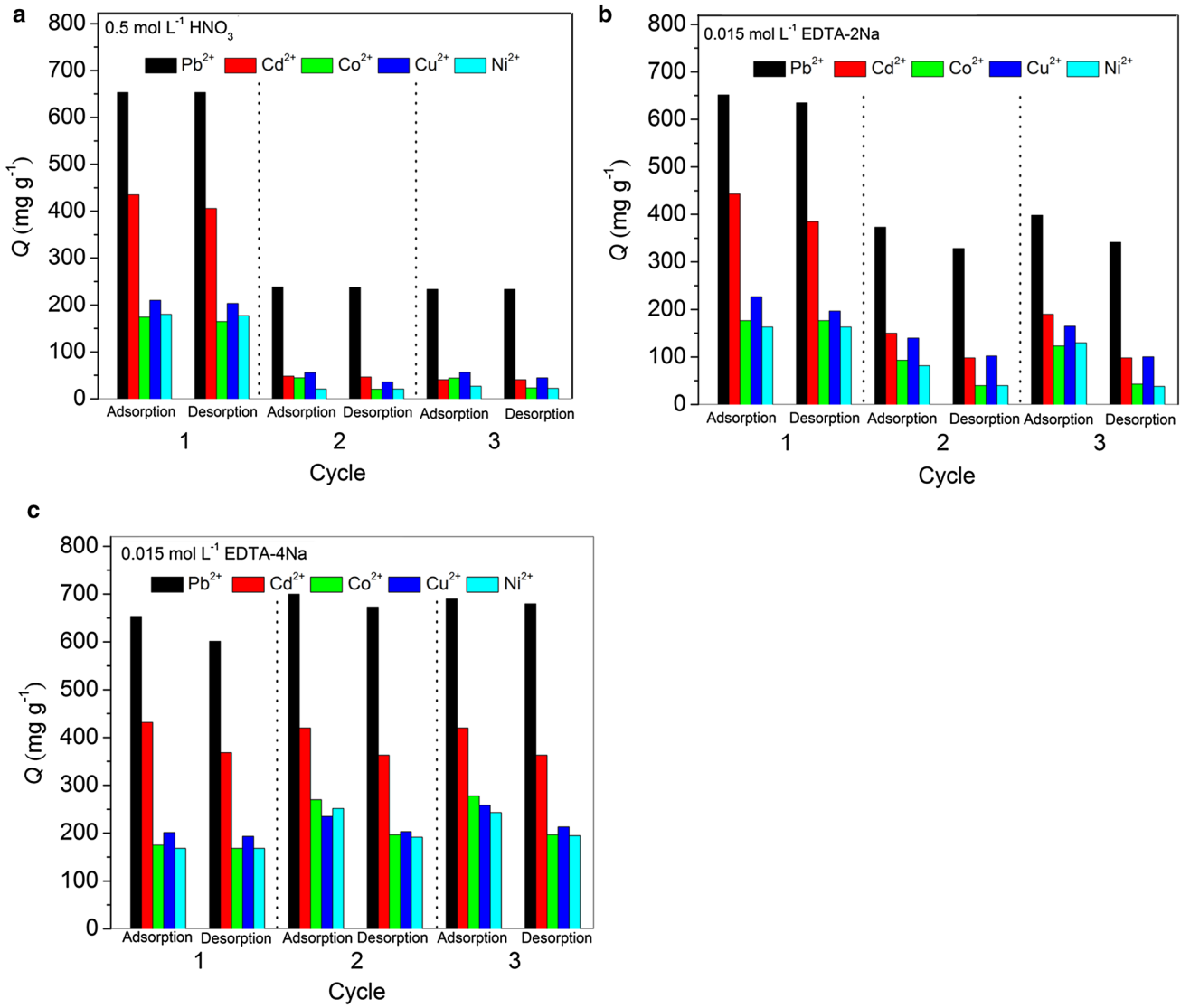

Fig. 3 Adsorption and desorption capacities of heavy-metal ions in: **a** 0.5 mol L^{-1} HNO_3; **b** 0.015 mol L^{-1} EDTA-2Na; and **c** 0.015 mol L^{-1} EDTA-4Na solutions at three cycles

and EDTA-4Na are known as very strong chelating agents for many heavy metals, it is thought to replace the active groups on the adsorbent and to make complex with heavy-metal ions. The larger stability constant can produce higher desorption ratio. In addition, the desorption is an ion-exchange process between Na^+ and heavy-metal ions, so, for the absorbed heavy-metal ions, desorption can occur in EDTA-2Na and EDTA-4Na solutions [31]. HNO_3, as an eluent, shows good proton-exchange process because it can change the stability constant between adsorbent and heavy-metal ions. The stronger the acidity, the lower would be the coordination strength. Consequently, HNO_3, EDTA-2Na and EDTA-4Na were chosen as the eluents for desorption of heavy-metal ions.

To examine the reusability of the adsorbent, sequential adsorption–desorption cycles were repeated three times using 0.5 mol L^{-1} HNO_3, 0.015 mol L^{-1} EDTA-2Na and 0.015 mol L^{-1} EDTA-4Na solutions as the eluents, respectively. The adsorption and desorption capacities at each cycle are shown in Fig. 3. The adsorption capacities decrease from one cycle to another using HNO_3 (a) and EDTA-2Na (b) as eluents. However, the adsorption capacities are almost maintained similar for three cycles in EDTA-4Na solution (c) as eluent. That is to say, all heavy-metal ions show high adsorption and desorption capacities in their third adsorption–desorption cycle using EDTA-4Na solution as eluent. This suggests that neutral EDTA-4Na eluent is better for desorption of heavy-metal ions than

Table 3 Desorption ratio (%) at sequential three adsorption–desorption cycles using 0.5 mol L^{-1} HNO_3, 0.015 mol L^{-1} EDTA-2Na and 0.015 mol L^{-1} EDTA-4Na as eluents

Eluents	Cycle	Desorption ratio (%)				
		Pb^{2+}	Cd^{2+}	Co^{2+}	Cu^{2+}	Ni^{2+}
0.5 mol L^{-1} HNO_3	1	100.0	93.3	94.7	96.8	98.6
	2	99.7	96.5	46.3	64.3	100.0
	3	100.0	100.0	53.0	79.2	84.3
0.015 mol L^{-1} EDTA-2Na	1	97.4	86.8	100.0	86.8	100.0
	2	87.9	65.5	42.9	72.9	49.0
	3	85.8	51.7	34.9	60.8	29.5
0.015 mol L^{-1} EDTA-4Na	1	92.1	85.3	96.2	95.9	100.0
	2	96.2	86.5	72.9	86.5	76.2
	3	98.6	86.5	70.7	82.7	80.1

EDTA-2Na (a weak acid) and HNO_3. After desorption by EDTA-2Na and HNO_3, the active groups such as $–COO^-$ and $–SO_3^-$ on the adsorbent are protonated to –COOH and $–SO_3H$ which block the further chelation interactions between these groups and heavy-metal ions because of hydrogen-bond interactions. Moreover, we also found that the adsorbent exhibited a slight dissolution or mass loss in the second cycle in HNO_3 solution. In addition, HNO_3 causes strong corrosion in equipments. Therefore, it is concluded that EDTA-4Na is a promising eluent for the adsorbent which has absorbed heavy-metal ions, and the EDTA-4Na solution is probably more suitable in long-term usage.

The desorption ratio of EDTA-4Na, EDTA-2Na and HNO_3 at consecutive three adsorption–desorption cycles are listed in Table 3. It can be observed that Pb^{2+} ions show over 85% desorption ratio in each adsorption–desorption cycle in different eluents. Cd^{2+}, Co^{2+}, Cu^{2+} and Ni^{2+} ions also show certain desorption ratios in HNO_3 and EDTA-2Na solutions at the second and third cycles. According to the data of Table 3, we take it for granted that EDTA-2Na and HNO_3 also have good performance for desorption of heavy metal ions. However, this conclusion is incorrect based on Fig. 3 because desorption ratio is only a value which does not reflect the true characteristic of adsorption–desorption process with certainty. For example, if the second adsorption capacities are low and the desorption capacities are high, then, desorption ratio can reach to 95%. So the given desorption ratio has a few limitations during the study of regeneration and reusability. Only when the adsorbent has high adsorption and desorption capacity in consecutive cycles, the adsorbent would be promising in regeneration performance.

Selective adsorption of Pb^{2+} on CS/P(AMPS-*co*-AA) adsorbent

Competitive adsorption kinetics of Pb^{2+}, Cd^{2+}, Co^{2+}, Cu^{2+} and Ni^{2+} onto CS/P(AMPS-*co*-AA) adsorbent at the concentrations of 300 and 1.45 mmol L^{-1} were determined (simultaneous adsorption from solutions containing all the metal ions) at pH 4.8 and 25 °C, respectively. Figure 4 shows the kinetics curves of competitive adsorptions at two different units of adsorption capacities, such as mass adsorption capacities (mg g^{-1}, Fig. 4a, b) and molar adsorption amount (mmol g^{-1}, Fig. 4c, d). In all the four cases, Pb^{2+} ion adsorption capacities increase with the adsorption time. On the contrary, other ions are found to be adsorbed at initially 20 min, but then the adsorption capacities gradually decrease and, finally, become almost negligible for Co^{2+} and Ni^{2+} after 180 min. Obviously, the initially adsorbed Cd^{2+}, Co^{2+}, Cu^{2+} and Ni^{2+} ions on the adsorbent are subsequently released from the adsorbent into the solution in the competitive adsorption process. When the adsorbent was added into the mixture solution, all metal ions had the opportunities to occupy the chelating sites because a large number of unreacted chelating groups existed in the adsorbent. When the chelating sites were occupied by adsorbed heavy-metal ions, no metal ions could diffuse toward the adsorption sites except Pb^{2+}. The result suggested that the coordination bonds between chelating group and Pb^{2+} are more stable than those between chelating group and Cd^{2+}, Co^{2+}, Cu^{2+} and Ni^{2+}. When the Pb^{2+} ions diffuse into the chelating sites of hydrogel, they can replace other adsorbed heavy-metal ions [32]. Therefore, the adsorption capacity of Pb^{2+} is gradually increased, and the adsorption capacity of other heavy-metal ions is increased first and then dropped over time until zero point for Co^{2+} and Ni^{2+}. That is, the adsorbent has outstanding selective adsorption for Pb^{2+} after a proper adsorption time.

Under the equal initial mass concentration of each metal ion (300 mg L^{-1}, Fig. 4a), the number of ions ratio is not equal and the order of ions ratio from high to low is Ni^{2+} > Co^{2+} > Cu^{2+} > Cd^{2+} > Pb^{2+}, because the order of relative atomic mass is Pb^{2+} > Cd^{2+} > Cu^{2+} > Co^{2+} > Ni^{2+}. However, under the equal molar concentrations at initial stage (1.45 mmol L^{-1}, Fig. 4b), the number of ionic ratio

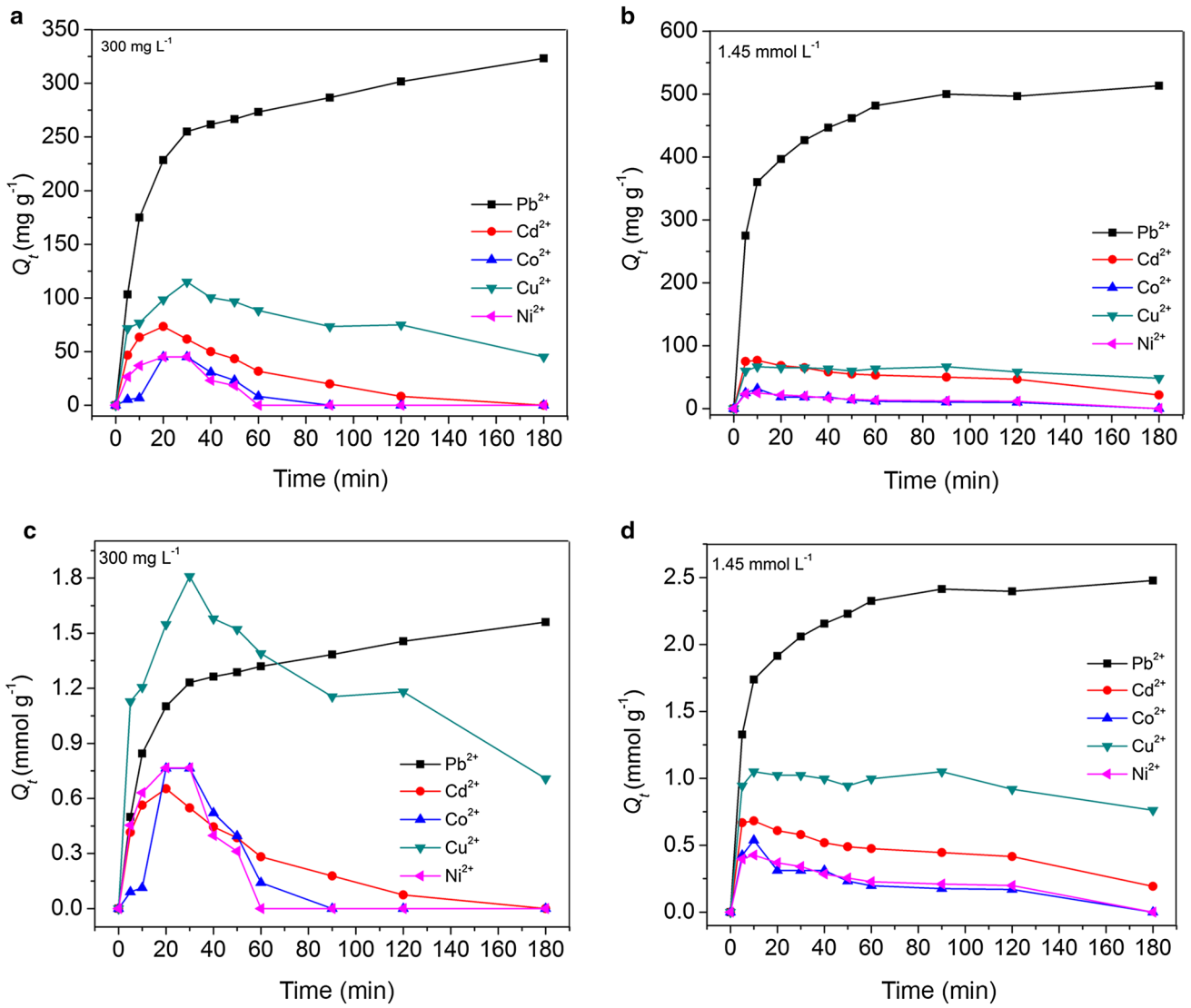

Fig. 4 Competitive adsorptions at initial equal concentrations of Pb^{2+}, Cd^{2+}, Co^{2+}, Cu^{2+} and Ni^{2+} (**a, c** 300 mg L^{-1} and **b, d** 1.45 mmol L^{-1}) at pH 4.8

would be equal as well. Koong et al. [33] found that the adsorption capacity of the heavy-metal ions increased with higher ratio of the metal ions. Thus, the maximum adsorption capacity of Pb^{2+} in Fig. 4a is lower and other adsorption capacities are higher than those in Fig. 4b. In addition, the adsorption kinetics of Pb^{2+} does not reach equilibrium up to 180 min and the adsorption capacities of the Cd^{2+}, Co^{2+}, Cu^{2+} and Ni^{2+} continue to slow down after 20 min (Fig. 4a). This is an indication that the ionic ratio will affect the selective adsorption of metal ions and the result of selective adsorption is more reliable under the equal molar concentrations at the initial stage.

Because the adsorption process is directly related to the number of adsorption sites and metal ions, the units of each adsorption capacity converted from mass adsorption capacity (mg g^{-1}) to molar adsorption capacity (mmol g^{-1}) are shown in Fig. 4c, d. It is observed that the selectivity of CS/P(AMPS-*co*-AA) adsorbent for Pb^{2+} in Fig. 4c is not remarkable compared with Fig. 4a at 300 mg L^{-1}. However, Fig. 4d possibly reflects better the selective adsorption of adsorbent for Pb^{2+} compared with Fig. 4c. This further illustrates that the ionic ratio greatly affects the selectivity adsorption. In Fig. 4b the adsorbent exhibits good selectivity of Pb^{2+} in mixture solution, while the order of other ions is closely mixed, especially Cu^{2+} and Cd^{2+}. However, we can clearly see in Fig. 4d that the order of selective adsorption is $Pb^{2+} > Cu^{2+} > Cd^{2+} > Co^{2+} \approx Ni^{2+}$. This further illustrates that conversion unit of adsorption capacities from mg g^{-1} to mmol g^{-1} is very necessary. This result suggests that equal molar concentration

(mol L^{-1}) and molar adsorption capacities (mmol g^{-1}) are more accurate and reliable for studying the selective adsorption.

CS/P(AMPS-*co*-AA) adsorbent is a cross-linked, three-dimensional polymer (Fig. S3 in supplementary material) which has a very complicated structure. Stability constants of metal ions are not obtained experimentally due to lack of actual complexation data between heavy-metal ions and surface functional groups. If one heavy-metal ion complex is more stable than another of the same type, a heavy-metal ion will displace another from a less stable complex [34]. Irving and Williams [35] found that the stability of complexes for the first transition series followed the order: $Mn^{2+} < Fe^{2+} < Co^{2+} < Ni^{2+} < Cu^{2+} > Zn^{2+}$. Figure 4d shows that the stability of adsorption of metal ions follows the order: $Pb^{2+} > Cu^{2+} > Cd^{2+} > Co^{2+} \approx Ni^{2+}$. So Cu^{2+}, Co^{2+} and Ni^{2+} ions correspond to the order of the Irving–Williams series. In addition, the ionic radius of Pb^{2+} ion (1.21 Å) is larger than that of Cu^{2+} (0.72 Å), Cd^{2+} (0.97 Å), Co^{2+} (0.72 Å) and Ni^{2+} (0.69 Å), and thus a stronger physical affinity for Pb^{2+} is expected for binding sites on the adsorbent [36]. It is indicated that the CS/P(AMPS-*co*-AA) adsorbent has a good adsorption selectivity for Pb^{2+} with the coexistence of Cu^{2+}, Cd^{2+}, Co^{2+} and Ni^{2+} ions. Therefore, the CS/P(AMPS-*co*-AA) adsorbent can be applied in separation of Pb^{2+} in aqueous systems containing Cu^{2+}, Cd^{2+}, Co^{2+}, Ni^{2+} ions.

Adsorption mechanism

XPS spectra are a useful tool in exploring the adsorption mechanism [37, 38]. Figure 5 shows the XPS spectra for the adsorbent before and after adsorption of Pb^{2+}. It is obvious that the peaks of Na(A) (binding energy = 497.9 eV) and Na1s (binding energy = 1072.0 eV) completely disappear. The Pb5d (binding energy = 21.4 eV), Pb4f (binding energy = 142.7 eV), Pb4d (binding energy = 412.8, 434.8 eV) and Pb4p (binding energy = 644.5 eV) peaks appear in the spectra of the adsorbent after adsorption of Pb^{2+}. This indicates that Na^+ ions are exchanged with the Pb^{2+} ions during the adsorption process [37, 39]. In addition, it is noticeable that the binding energy (399.7 eV) of N1s has quite a large shift towards higher binding energies (400.0 eV) after adsorption of Pb^{2+} (Fig. S5 in supplementary material). This is due to the formation of a complex through a coordinated covalent bond, in which a lone pair of electrons in the N atom is donated to the shared bond between N and Pb^{2+}. As a consequence, the electron cloud density of the N is reduced, and thus a higher binding energy is observed [37, 40]. The possible interaction mechanism between the CS/P(AMPS-*co*-AA) hydrogel and Pb^{2+} is shown in Scheme 1.

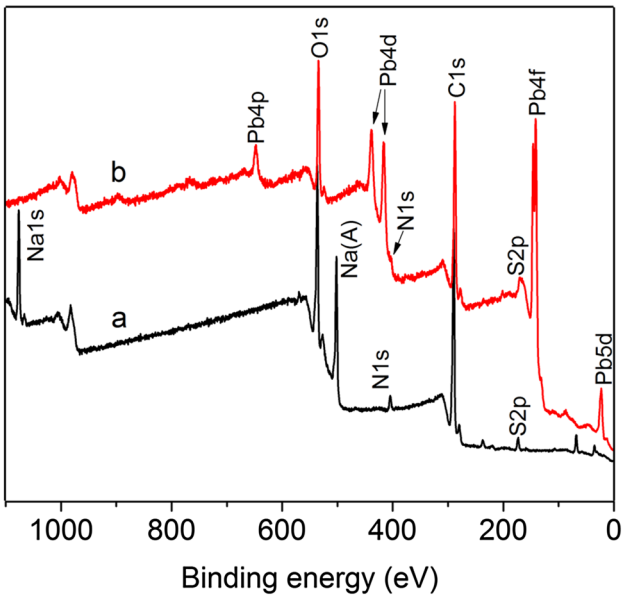

Fig. 5 XPS spectra of the CS/P(AMPS-*co*-AA) adsorbent: **a** before and **b** after adsorption of Pb^{2+}

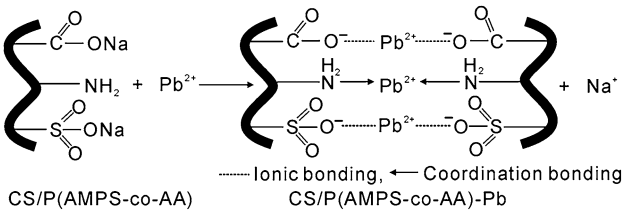

Scheme 1 Possible interaction mechanism between CS/P(AMPS-*co*-AA) adsorbent and Pb^{2+}

Conclusion

The CS/P(AMPS-co-AA) adsorbent was successfully synthesized by one-step grafting polymerization and crosslinking reaction of CS, AMPS and AA in aqueous solution using glow discharge electrolysis plasma technique. The XPS analysis suggested the ion-exchange between Na^+ and Pb^{2+}, and the chemical complexation between Pb^{2+} and $–NH_2$ groups for the mechanism of adsorption of Pb^{2+}. The optimum pH for the adsorption of Pb^{2+}, Cd^{2+}, Co^{2+}, Cu^{2+} and Ni^{2+} was 4.8, and time of adsorption equilibrium was achieved in 180 min. The equilibrium adsorption capacities of Pb^{2+}, Cd^{2+}, Co^{2+}, Cu^{2+}, and Ni^{2+} at pH 4.8 and 25 °C corresponded to 673.3, 358.3, 176.7, 235.0 and 171.7 mg g^{-1}. Adsorption kinetics of heavy metal ions on the adsorbent fitted well to the pseudo second-order model. The adsorbent displayed excellent regeneration and reusability using 0.015 mol L^{-1} EDTA-4Na solution as the

eluent. The desorption ratio could not correctly reflect the true characteristic of adsorption–desorption process. The CS/P(AMPS-*co*-AA) adsorbent showed a promising adsorption selectivity toward Pb^{2+} with the coexistence of Cd^{2+}, Co^{2+}, Cu^{2+}, and Ni^{2+} ions. During the process of selective adsorption, the molar adsorption capacity of all metal ions, at equal molar concentration in the initial stage, was more reliable than their mass adsorption capacity. All the results indicated that the CS/P(AMPS-*co*-AA) adsorbent revealed large adsorption capacities, promising regeneration, and high selectivity for Pb^{2+}. Therefore, it seems to have a high potential as a very promising absorbent for the separation, purification and selective recovery of Pb^{2+} in aqueous systems containing Cd^{2+}, Co^{2+}, Cu^{2+}, and Ni^{2+} ions.

Acknowledgements This work was supported by National Natural Science Foundation of China (Nos. 21367023, 21567025 and 11564037).

References

1. Liu YM, Ju XJ, Xin Y, Zheng WC, Wang W, Wei J, Xie R, Liu Z, Chu LY (2014) A novel smart microsphere with magnetic core and ion-recognizable shell for Pb^{2+} adsorption and separation. ACS Appl Mater Interfaces 6:9530–9542
2. Gunathilake C, Kadanapitiye MS, Dudarko O, Huang SD, Jaroniec M (2015) Adsorption of lead ions from aqueous phase on mesoporous silica with P-containing pendant groups. ACS Appl Mater Interfaces 7:23144–23152
3. Ali I (2012) New generation adsorbents for water treatment. Chem Rev 112:5073–5091
4. Ali I (2014) Water treatment by adsorption columns: evaluation at ground level. Sep Purif Rev 43:175–205
5. van Kuringen HPC, Eikelboom GM, Shishmanova IK, Broer DJ, Schenning APHJ (2014) Responsive nanoporous smectic liquid crystal polymer networks as efficient and selective adsorbents. Adv Funct Mater 24:5045–5051
6. Ali I, Gupta VK (2006) Advances in water treatment by adsorption technology. Nat Protoc 1:2661–2667
7. Li K, Wang Y, Huang M, Yan H, Yang H, Xiao S, Li A (2015) Preparation of chitosan-graft-polyacrylamide magnetic composite microspheres for enhanced selective removal of mercury ions from water. J Colloid Interface Sci 455:261–270
8. Pan YF, Cai PX, Farmahini-Farahani M, Li YD, Hou XB, Xiao HN (2016) Amino-functionalized alkaline clay with cationic star-shaped polymer as adsorbents for removal of Cr(VI) in aqueous solution. Appl Surf Sci 385:333–340
9. Wang X, Chung YS, Lyoo WS, Min BG (2006) Preparation and properties of chitosan/poly(vinyl alcohol) blend foams for copper adsorption. Polym Int 55:1230–1235
10. Zhou L, Shang C, Liu Z, Huang G, Adesina AA (2012) Selective adsorption of uranium(VI) from aqueous solutions using the ion-imprinted magnetic chitosan resins. J Colloid Interface Sci 366:165–172
11. Petrova YS, Pestov AV, Usoltseva MK, Neudachina LK (2015) Selective adsorption of silver(I) ions over copper(II) ions on a sulfoethyl derivative of chitosan. J Hazard Mater 299:696–701
12. Zhang M, Helleur R, Zhang Y (2015) Ion-imprinted chitosan gel beads for selective adsorption of Ag^{+} from aqueous solutions. Carbohydr Polym 130:206–212
13. Zhang M, Zhang Y, Helleur R (2015) Selective adsorption of Ag^{+} by ion-imprinted *O*-carboxymethyl chitosan beads grafted with thiourea-glutaraldehyde. Chem Eng J 264:56–65
14. Lin S, Wei W, Wu X, Zhou T, Mao J, Yun YS (2015) Selective recovery of Pd(II) from extremely acidic solution using ion-imprinted chitosan fiber: adsorption performance and mechanisms. J Hazard Mater 299:10–17
15. Chen X, Lam KF, Mak SF, Yeung KL (2011) Precious metal recovery by selective adsorption using biosorbents. J Hazard Mater 186:902–910
16. Li K, Gao Q, Yadavalli G, Shen X, Lei H, Han B, Xia K, Zhou C (2015) Selective adsorption of Gd^{3+} on a magnetically retrievable imprinted chitosan/carbon nanotube composite with high capacity. ACS Appl Mater Interfaces 7:21047–21055
17. Yan H, Dai J, Yang Z, Yang H, Cheng R (2011) Enhanced and selective adsorption of copper(II) ions on surface carboxymethylated chitosan hydrogel beads. Chem Eng J 174:586–594
18. Li X, Wang Z, Li Q, Ma J, Zhu M (2015) Preparation, characterization and application of mesoporous silica-grafted graphene oxide for highly selective lead adsorption. Chem Eng J 273:630–637
19. Laus R, Costa TG, Szpoganicz B, Favere VT (2010) Adsorption and desorption of Cu(II), Cd(II) and Pb(II) ions using chitosan crosslinked with epichlorohydrin-triphosphate as the adsorbent. J Hazard Mater 183:233–241
20. Vetriselvi V, Santhi RJ (2015) Redox polymer as an adsorbent for the removal of chromium(VI) and lead(II) from the tannery effluents. Water Resour Ind 10:39–52
21. Wan Ngah WS, Teong LC, Toh RH, Hanafiah MAKM (2012) Utilization of chitosan-zeolite composite in the removal of Cu(II) from aqueous solution: adsorption, desorption and fixed bed column studies. Chem Eng J 209:46–53
22. Xu YY, Dang QF, Liu CS, Yan JQ, Fan B, Cai JP, Li JJ (2015) Preparation and characterization of carboxyl-functionalized chitosan magnetic microspheres and submicrospheres for Pb^{2+} removal. Colloid Surf A 482:353–364
23. Zhang Y, Qu RJ, Sun CM, Ji CN, Chen H, Yin P (2015) Improved synthesis of silica-gel-based dendrimer-like highly branched polymer as the Au(III) adsorbents. Chem Eng J 270:110–121
24. Chen AH, Yang CY, Chen CY, Chen CW (2009) The chemically crosslinked metal-complexed chitosans for comparative adsorptions of Cu(II), Zn(II), Ni(II) and Pb(II) ions in aqueous medium. J Hazard Mater 163:1068–1075
25. Yu J, Li Y, Lu QF, Zheng JD, Yang SX, Jin F, Wang QZ, Yang W (2016) Synthesis, characterization and adsorption of cationic dyes by CS/P(AMPS-co-AM) hydrogel initiated by glow-discharge-electrolysis plasma. Iran Polym J 25:423–435
26. Yu J, Zhang HT, Li Y, Lu QF, Wang QZ, Yang W (2016) Synthesis, characterization, and property testing of PGS/P(AMPS-*co*-AM) superabsorbent hydrogel initiated by glow-discharge electrolysis plasma. Colloid Polym Sci 294:257–270
27. Yu J, Yang GG, Pan YP, Lu QF, Yang W, Gao JZ (2014) Poly(acrylamide-*co*-acrylic acid) hydrogel induced by glow-discharge-electrolysis plasma and its adsorption properties for cationic dyes. Plasma Sci Technol 16:767–776
28. Heidari A, Younesi H, Mehraban Z, Heikkinen H (2013) Selective adsorption of Pb(II), Cd(II), and Ni(II) ions from aqueous solution using chitosan-MAA nanoparticles. Int J Biol Macromol 61:251–263
29. Li Z, Xiao D, Ge Y, Koehler S (2015) Surface-functionalized porous lignin for fast and efficient lead removal from aqueous solution. ACS Appl Mater Interfaces 7:15000–15009
30. Kabiri S, Tran DN, Azari S, Losic D (2015) Graphene-diatom silica aerogels for efficient removal of mercury ions from water. ACS Appl Mater Interfaces 7:11815–11823
31. Bessbousse H, Verchère JF, Lebrun L (2012) Characterisation of metal-complexing membranes prepared by the

semi-interpenetrating polymer networks technique: application to the removal of heavy metal ions from aqueous solutions. Chem Eng J 187:16–28
32. Chen CY, Chen SY (2004) Adsorption properties of a chelating resin containing hydroxy group and iminodiacetic acid for copper ions. J Appl Polym Sci 94:2123–2130
33. Koong LF, Lam KF, Barford J, McKay G (2013) A comparative study on selective adsorption of metal ions using aminated adsorbents. J Colloid Interface Sci 395:230–240
34. Irving H, Williams RJP (1948) Order of stability of metal complexes. Nature 162:746–747
35. Irving H, Williams RJP (1953) The stability of transition-metal complexes. J Chem Soc 8:3192–3210
36. Bayramoglu G, Yakup AM, Bektas S (2007) Removal of Cd(II), Hg(II), and Pb(II) ions from aqueous solution using P(HEMA/chitosan) membranes. J Appl Polym Sci 106:169–177
37. Wang WB, Huang DJ, Kang YR, Wang AQ (2013) One-step in situ fabrication of a granular semi-IPN hydrogel based on chitosan and gelatin for fast and efficient adsorption of Cu^{2+} ion. Colloids Surf B 106:51–59
38. Li ZY, Li TT, An LB, Liu H, Gu LN, Zhang ZM (2016) Preparation of chitosan/polycaprolactam nanofibrous filter paper and its greatly enhanced chromium(VI) adsorption. Colloids Surf A 494:65–73
39. Wan Ngah WS, Fatinathan S (2010) Pb(II) biosorption using chitosan and chitosan derivatives beads: equilibrium, ion exchange and mechanism studies. J Environ Sci 22:338–346
40. Lu QF, Yu J, Gao JZ, Yang W, Li Y (2011) Glow-discharge electrolysis plasma induced synthesis of polyvinylpyrrolidone/acrylic acid hydrogel and its adsorption properties for heavy-metal ions. Plasma Process Polym 8:803–814